Fluid Dynamics & Materials Processing

Tech Science Press

DOI: 10.32604/fdmp.2022.018972

ARTICLE

A Research on the Behavior of a Polyurethane Polymer Waterproof Material Used in Bridge Geotechnical Applications

Yuzhuo Wang[1,2] and Zhichao Xu[2,*]

[1]School of Agriculture and Hydraulic Engineering, Suihua University, Suihua, 152061, China

[2]Institute of Cold Regions Science and Engineering, Northeast Forestry University, Harbin, 150040, China

[*]Corresponding Author: Zhichao Xu. Email: zhichao199202@163.com

Received: 26 August 2021 Accepted: 23 November 2021

ABSTRACT

Polyurethane is enjoying a widespread use as a polymer-based waterproof material in civil engineering In the present study we consider a temperature-sensitive waterproof and moisture-permeable polyurethane material (PTPE-PU) characterized by one or more phase transition temperatures (critical temperatures). Near the critical temperature, the waterproof and moisture permeability of polyurethane undergo abrupt changes. The related stability, thermal performance, water resistance, hydrostatic pressure, and moisture permeability are investigated here considering a PTPE-PU traditionally used in bridge geotechnical engineering. The results show that the moisture permeability of the coated bridge rock and soil undergo sudden variations near the crystallization and melting temperature of the soft segment. The moisture permeability is 3000 g/(m^2d). The hydrostatic pressure of the coated bridge rock and soil is 3.5 kPa.

KEYWORDS

Polyurethane polymer; waterproof material; temperature-sensitive type; bridge foundation

1 Introduction

With modern science and technology, polyurethane as a new polymer material has developed rapidly in building waterproof materials. Its product types mainly include building waterproof coatings, building sealing materials, leak-stopping water-stop materials, rigid foam waterproof and thermal insulation materials, etc. These materials can be used for roof waterproofing, tunnel and underground engineering waterproofing, subway and ship waterproofing. If the water-swellable polyurethane waterproof material can absorb water and expand several times when it meets water, the gaps and holes can be blocked without leakage [1]. Polyurethane is used in construction projects for waterproofing, anti-seepage, plugging and caulking, because it has a good bonding ability to cement concrete, asphalt, wood, steel, and other materials. We use polyurethane high-analysis materials as waterproof materials in construction engineering and have a good future.

Temperature-sensitive polymers usually control the phase transition temperature and microphase separation structure of the material, making certain material properties responsive to temperature stimulation. The temperature-sensitive waterproof and moisture-permeable polyurethane has one or more phase transition temperatures (critical temperatures). In the vicinity of the critical temperature,

polyurethane's waterproof and moisture-permeable properties will undergo abrupt changes. There have been literature reports on synthesizing temperature-sensitive waterproof and moisture-permeable polyurethane materials, but most are solvent-based polyurethanes [2]. This substance has problems such as toxic, flammable, peculiar smell, high pollution, etc. Therefore, the research and preparation of water-based temperature-sensitive waterproof and moisture-permeable coating agents have become a hot topic.

Polyethylene glycol is considered to be a phase-inversion polymer with excellent properties and a moisture-transmitting factor. Scholars often use it in the synthesis of hydrophilic and moisture-conducting polyurethane [3]. Some scholars found that when the relative molecular weight of the polyethylene glycol segment in the polyurethane molecule is large, crystallization will occur when the solvent-based intelligent waterproof and moisture-permeable polyurethane is synthesized using polyethylene glycol as the blend polyether. Polytetrahydrofuran ether polyurethane membrane has a larger free volume, conducive to the diffusion and penetration of water vapor molecules. Therefore, this paper uses this as a raw material to prepare a synthetic water-based temperature-sensitive waterproof and moisture-permeable polyurethane bridge geotechnical coating agent that synergizes with hydrophilic, moisture-transmitting temperature-sensitive shape memory.

2 Experimental Part

2.1 Experimental Materials

The composition and melting point data of polyethylene glycol block polyester (PTPE) is shown in Table 1. Industrial grade isochrone diisocyanate (IPDI) from Bayer, Germany. Industrial-grade diethylpropion acid (DMPA) was vacuumed at 100°C for five h before use. Xilong Fine Chemical Co. Ltd.'s (Guangzhou, China) dibutyltin dilaurate is analytically pure. The 1,4-butanediol (BDO) analytical grade of Xilong Fine Chemical Co., Ltd. (Guangzhou, China) was soaked in 4A molecular sieve for seven days before use. The methyl ethyl ketone (MEK) analytical grade of Xilong Fine Chemical Co. Ltd. (Guangzhou, China) was soaked with 4A molecular sieve for seven days before use. TF601 thickener and polyester spun fabric provided by Zhejiang Transcend Co., Ltd. (China). Commercially available triethylamine (TEA) analytical reagents can be used directly.

Table 1: Composition and characteristics of PTPE

Sample	n(PTMG):n(PEG)	Average molecular weight	Melting point (Ts)/°C
PT10PE2	1:1(PTMG1000:PEG200)	3355	20, 30
PT10PE6	1:1(PTMG1000:PEG600)	3677	22, 29
PT10PE10	1:1(PTMG1000:PEG1000)	4256	42
PT10PE20	1:1(PTMG1000:PEG2000)	4415	41, 58
PT20-PE6	1:1(PTMG2000:PEG600)	4556	37
PT20-PE10	1:1(PTMG2000:PEG1000)	4232	38

2.2 Preparation of Polyurethane Prepolymer and Its Water Dispersion

We put the block polyether PTPE in a four-necked flask equipped with a stirring and refluxing condensing device according to the formula listed in Table 2. The temperature was raised to 100°C, and the vacuum was applied to remove water for 3 h. We lower the temperature to 60°C to 70°C and then release the vacuum to pass nitrogen [4]. We add IPDI/MEK (3/1) dropwise to the bottle and raise the temperature to 80°C for 1 h. In the experiment, dibutyltin dilaurate was added dropwise to the system. Its mass is 0.05% of the polyether mass. After continuing the reaction for 1 h, we drop in DMPA and BDO successively and continue to react for 3 to 5 h. Then, the temperature was lowered to 50°C, and TEA was added to neutralize the reaction for 0.5 h to prepare PTPE-PU prepolymer. Then we shear the prepolymer

at high speed in water for 5–10 min to obtain a PTPE-PU emulsion with a solids content of 15%. The synthesis process of PTPE-PU is shown in Fig. 1.

Table 2: Symbols and composition of PTPE-PU

Sample	n(IPDI)/mol	n(PTPE)/mol	n(BDO)/mol	n(DMPA)/mol	n(TEA)/mol
PT10PE2-PU	0.1253	0.01937	0.0515	0.01866	0.01959
PT10PE6-PU	0.1248	0.01768	0.05281	0.01866	0.01959
PT10PE10-PU	0.1241	0.01527	0.05468	0.01866	0.01959
PT10PE20-PU	0.1239	0.01472	0.05511	0.01866	0.01959
PT20PE6-PU	0.1237	0.01427	0.05546	0.01866	0.01959
PT20E10-PU	0.1241	0.0154	0.05458	0.01866	0.01959

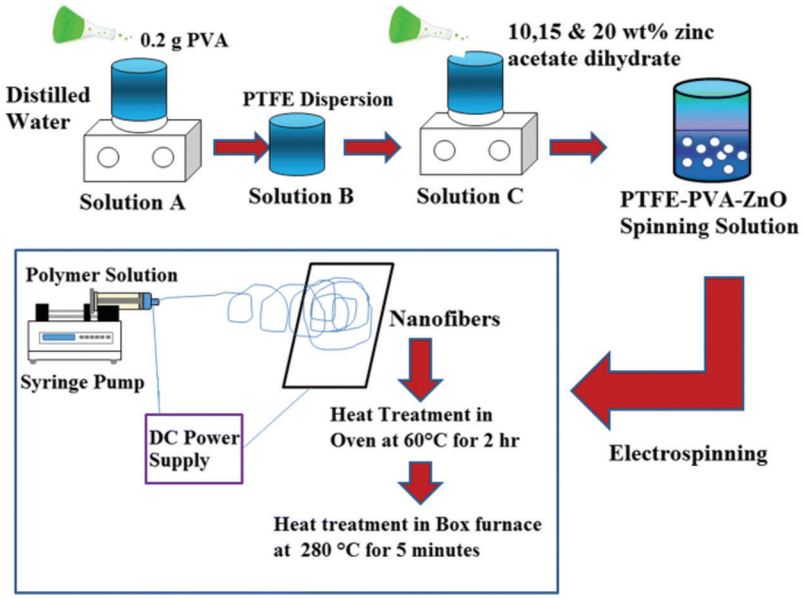

Figure 1: Synthesis process of PTPE-PU

2.3 Preparation of Membrane Samples and Coated Bridge Geotechnical Samples

We cast the PTPE-PU emulsion into a film in a polytetrafluoroethylene mold, dry it naturally for seven days, and place it in a vacuum oven at 60°C to vacuum dry to a constant amount. Add 1% mass fraction of TF601 thickener to PTPE-PU emulsion for thickening [5]. We use an LTE-S79507 type coating machine for geotechnical coating. The coating and baking temperature is 170°C, the coating and baking time is 45 s, and the coating film thickness is 80–100 μm.

2.4 Structure and Performance Characterization

2.4.1 Structural Characterization of PTPE-PU-Infrared Spectroscopy (FT-IR)

The experiment uses a methyl ethyl ketone-n-hexane solvent system to purify PTPE-PU prepolymer and uses AVATAR360 Fourier transform infrared spectrometer to measure.

2.4.2 Stability of PTPE-PU Emulsion-Determination of Particle Size and Zeta Potential

In the experiment, the WFSPU emulsion was diluted to 1% and measured at 25°C using a ZS90 nanoparticle size and Zeta potential analyzer.

2.4.3 Microstructure of PTPE-PU Film-DSC Measurement

We weighed about 10 mg of the film sample and tested it with a Mettler DSC1 differential scanning calorimeter. The experiment was heated in a nitrogen atmosphere at a heating rate of 10 °C/min.

2.4.4 Test of Mechanical Properties of PTPE-PU Film

The experiment uses an AGS-J type mechanical testing machine to test according to GB/T1040-79.

2.4.5 Waterproof and Moisture Permeability Test of Coated Bridge Rock and Soil

We use a water permeability tester following the GB/T4744-1997 standard for hydrostatic pressure test; use a bridge rock and soil permeability tester following GB/T12704-91 standard A method (positive cup method) to determine the moisture permeability.

3 Results and Discussion

3.1 Infrared Characterization of PTPE-PU

Fig. 2 shows the infrared spectrum of PTPE-PU. It can be seen from the figure that there is no hydroxyl absorption peak near 3481 cm^{-1}. The absorption peaks of 3321 cm^{-1} and 1530 cm^{-1} are attributed to the N-H bond's stretching and bending vibrations in the urethane bond. The absorption peaks at 2943 cm^{-1}, 2854 cm^{-1}, and 2796 cm^{-1} are attributed to the C-H stretching vibration peaks in methyl-CH^{2-}. 2261 cm^{-1} is attributed to the characteristic absorption peak of residual-NCO (R > 1). The characteristic absorption peak of C=O stretching vibration in the urethane bond appeared at 1716 cm^{-1}. 1108 cm^{-1} is the characteristic peak of C-O-C stretching vibration. The above shows that -NCO in isocyanate has reacted with -OH in PTPE to form polyurethane.

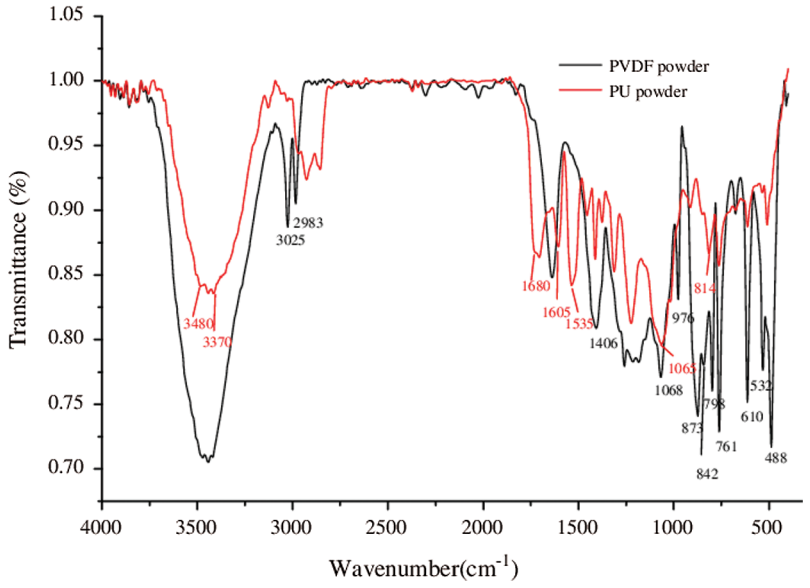

Figure 2: FT-IR spectrum of PTPE-PU

3.2 Stability of PTPE-PU Water Dispersion

To investigate the stability of the PTPE-PU water dispersion, we placed the emulsion for three months and observed the appearance of the emulsion. We measure the particle size and Zeta potential of the emulsion. Table 3 shows the observation and test results of the emulsion. From the data in the table, it can be seen that the particle size of the PTPE-PU series emulsion is nanometer, the particle size distribution parameter PDI value is small, and there is little change between the emulsions. The absolute value of the zeta potential of each emulsion is greater than 30 mV. The above shows that the synthesized PTPE-PU emulsion has a good particle size monodispersed, and its water dispersion system is stable. It is found through observation that the PT10PE20-PU emulsion has fluidity after emulsification [6]. After 1d, the emulsion becomes unable to flow, making it impossible to coat the rock and soil of the bridge. The reason is that the PEG content in the polyurethane is too high, and its ability to associate with water becomes stronger.

Table 3: Appearance, size, particle size distribution coefficient, and zeta-potential of PTPE-PU emulsion

Sample	Emulsion appearance	Z-average size (r)/nm	Pdi	Zeta potential/mV
PT10PE2-PU	Semitransparent, blue	90.1	0.138	−41.0
PT10PE6-PU	Semitransparent, colorless	88.3	0.145	−42.8
PT10PE10-PU	Semitransparent, colorless	72.8	0.142	−46.7
PT10PE20-PU	Semitransparent, colorless, mobility-lost	84.5	0.136	−48.3
PT20PE6-PU	Semitransparent, blue	93.2	0.14	−43.3
PT20E10-PU	Semitransparent, colorless	78.4	0.142	−45.7

3.3 Thermal Properties of PTPE-PU Film

Fig. 3 is the DSC curve of PTPE-PU. It can be seen from the figure that each PTPE-PU has a glass transition around −80°C. In addition, a small melting peak appeared on the DSC curves of PT20PE10-PU and PT20PE6-PU, and the exothermic enthalpies were 0.47 J/g and 0.66 J/g, respectively. A larger crystal melting peak appeared in the DSC curve of PT10PE10-PU, and the exothermic enthalpy was 15.24 J/g. The other two types of polyurethane films did not show a crystalline melting peak. It can be seen that although the soft segment itself has a strong crystallization ability, the symmetry and regularity of the molecular chain are reduced after the reaction produces anionic polyurethane [7]. The intermolecular force increases, and the molecular flexibility decreases. Excessive -NCO chain extension in water will also generate a micro-crosslinked structure, which will greatly reduce the crystallization ability of polyurethane after curing into a film. Only several polyurethanes with strong crystallization ability have crystallization behavior. And only when the two kinds of block polyether molecular chain length reach the optimal ratio can the polyurethane with higher crystallinity be obtained.

3.4 The Relationship between the Free Volume Cavity of PTPE-PU Film and Moisture Permeability

Positron Annihilation Lifetime Spectroscopy (PALS) is a sensitive microprobe to study the microstructure changes of amorphous polymers. The triplet positron o-Ps are localized in the free volume of the polymer and annihilated in the form of pick-off. o-Ps annihilation life (τ_3) and strength (I_3) are closely related to the free volume void of the polymer. We can use the semi-empirical formula (1) to calculate the average radius R of the free volume cavity through the positron annihilation spectrum to obtain and related information. According to formula (2) and formula (3), the relative free volume fraction in the polymer can be obtained, and then the free volume void size of the PTF-PUPU film can be calculated.

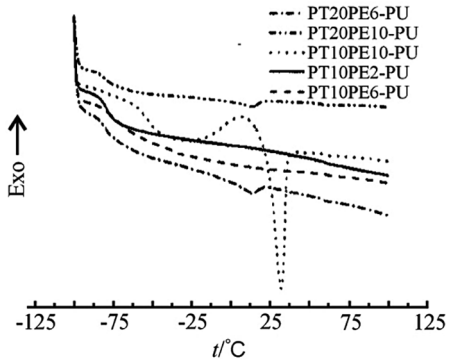

Figure 3: DSC analysis for PTPE-PU films

The above experiment can investigate the change of polyurethane microstructure with temperature.

$$\tau_3 = \frac{1}{2}[1 - \frac{R}{R_0} + \frac{1}{2\pi}\sin(\frac{2\pi R}{R_0})]^{-1} \tag{1}$$

$$V_h = 4\pi R^3/3 \tag{2}$$

$$f_v/C = V_h I_3 \tag{3}$$

Among them $R_0 = R + \delta_R, \delta_R$ is the fitting constant and $\delta_R = 0.166\,nm$.

Fig. 4 is the change curve of the free volume of each PTPE-PU film with temperature. It can be seen from the figure that the free volume radius of the PTPE-PU film gradually increases with the increase of temperature. Among them, the free volume radius of PT10PE2-PU, PT10PE6-PU, PT20PE6-PU, and PT20PE10-PU increase sequentially. The four types of polyurethane have similar changes with temperature. The free volume radius of PT10PE10-PU increases with temperature larger than the previous three types. When the temperature increased from 25°C to 38°C, the free volume radius jumped sharply. The changes in the free volume of the first four types of polyurethanes are all caused by the high elastic thermal expansion effect.

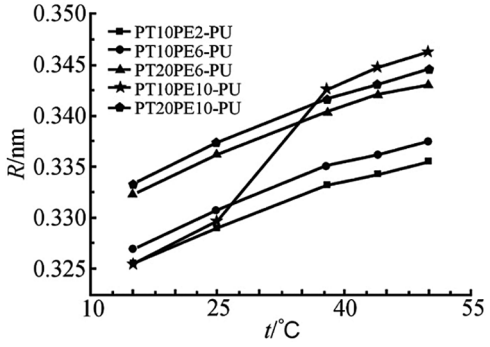

Figure 4: Average free volume of PTPE-PU

Although PT20PE6-PU and PT20PE10-PU polyurethane films also have phase changes, their melting point is about 13°C. Below 15°C and the crystallinity is small. Above 15°C, it is mainly amorphous and highly elastic volume thermal expansion. The energy of the thermal motion of the polymer increases, and the rotational motion within the molecule and the conformational change of the chain segment become

more active [8]. The increase in the degree of disorder within the molecule leads to an increase in the free volume of the highly elastic amorphous polymer. Hence, its free volume change is equivalent to that of the other two amorphous polyurethanes. PT10PE10-PU has a higher melting point. As the temperature rises, the crystalline part of the crystalline polymer melts. Its melting point is much lower than its viscous flow temperature, and it does not become a dense flow state after melting. The movement of the chain segment of the crystal region is activated to cause a sudden jump in the free volume of the high-elastic polymer. When the temperature is higher than the polymer's melting point, its free volume change properties are the same as the other four polyurethanes, and the increase in free volume is similar.

3.5 Mechanical Properties of PTPE-PU Film

The first stretching process is equivalently expressed as:

$$F_\sigma(x) + kx = F_B(x) \tag{4}$$

F_σ represents the stress of the specimen when the strain is x. k is the equivalent elastic coefficient of the supporting spring. F_B is the tensile force measured by the force sensor. The secondary stretching process ends after the sample breaks. After that, the test piece and the force sensor are returned to their original positions for a second stretch to determine the elastic coefficient of the equivalent spring. This process can be expressed as:

$$kx = F_A(x) \tag{5}$$

F_A represents the displacement measured by the force sensor during the second stretching process, and the meaning of other parameters remains the same. According to formulas (4) and (5), the final calculation formula of stress and strain can be obtained as:

$$F_\sigma(x) = F_B(x) - F_A(x) \tag{6}$$

The application of the stretching force during the two stretching processes is realized by a stepping motor with a power spring sensor. The specific tension calculation formula is:

$$F = kf\,\delta. \tag{7}$$

kf is the elastic coefficient of the force sensor. The coefficient of elasticity has been optimized in the previous study and accurately calibrated in advance through experiments. Table 4 shows the tensile test data of PTPE-PU measured at 20°C. From the data in the table, it can be seen that the strength of PT10PE10-PU is significantly greater than the strength of the other four polyurethane films [9]. When the relative molecular mass of PTMG in PTPE-PU is the same, the polyurethane film with a larger PEG relative molecular mass has higher strength and lower elongation at break. However, when the relative molecular mass of PEG in PTPE-PU is the same, the relative molecular mass of PTMG is larger, and the elongation at break is also larger. PT10PE10-PU is a crystalline high-elastic polymer, and part of its polymer is in a crystalline state. Its molecules are arranged tightly, and the intermolecular forces are large, and it acts as a crosslinking point on the amorphous part. The material has poor flexibility. Under the action of tensile force, the polymer is difficult to deform. Compared with amorphous polymer, its mechanical strength is greater. When the relative molecular mass of PTMG in PT10PE10-PU is the same, the hydrogen bond between soft and hard segments with larger PEG relative molecular mass is stronger. This results in higher mechanical strength and lower elongation of the film.

Table 4: Mechanical properties of PTPE-PU films

Sample	Maximum tensile strength/Mpa	Elongation at break/%
PT10PE2-PU	16.89 ± 0.23	1050 ± 13
PT10PE6-PU	18.54 ± 0.22	994 ± 12
PT10PE10-PU	25.14 ± 0.23	815 ± 12
PT20PE6-PU	19.23 ± 0.24	1124 ± 13
PT20PE10-PU	20.10 ± 0.26	1268 ± 13

3.6 Waterproof and Moisture Permeability of PTPE-PU Coated Bridge Rock and Soil

Table 5 is the hydrostatic pressure data of the PTPE-PU coated bridge rock and soil. From the data in the table, it can be seen that as the relative molecular mass of PEG of the synthetic block polyether PTPE increases, the hydrostatic pressure of the coated bridge rock and soil gradually decreases. The hydrostatic pressure of PT10PE2-PU-coated bridge rock and soil is the largest [10]. The hydrostatic pressure of the PT10PE10-PU coated bridge rock and soil is 2.5 kPa. But when the relative molecular mass of PEG does not change. The hydrostatic pressure of the block polyether polyurethane synthesized with PTMG2000 is much higher than that of the PTMG1000 series. This can meet general taking requirements. In short, the waterproof ability of PTPE-PU series coatings is still relatively low. The main reason is that the PEG content in the polyurethane coating is high, and its affinity for water is strong. When there is pressure, water is easy to penetrate.

Table 5: Water permeability resistance of PTPE-PU bridge rock soil

Sample	PT10PE2-PU	PT10PE6-PU	PT10PE10-PU	PT20PE6-PU	PT20PE10-PU
HP/kPa	15.2	5.4	2.5	9.5	6.8

3.7 Moisture Permeability of PTPE-PU Coated Bridge Rock and Soil

Fig. 5 shows the variation curve of moisture permeability of PTPE-PU coated bridge rock and soil with temperature. It can be seen from the curve in the figure that as the temperature increases, the moisture permeability of each polyurethane-coated bridge rock and soil gradually increases. The curve trend is divided into three categories here. Among them, PT10PE2-PU and PT10PE6-PU are the first categories. PT20PE6-PU and PT20PE10-PU are the second categories. PT10PE10-PU is the third category [11]. When the temperature increases from 8°C to 18°C, the moisture permeability of the first category increases with the temperature, and there is a small jump in the moisture permeability. In contrast, the other two categories change slowly.

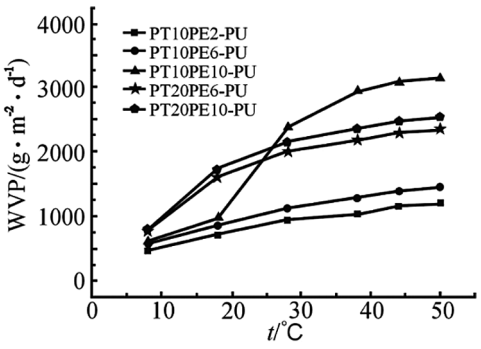

Figure 5: Moisture permeation property of PTPE-PU bridge rock soil

The reason is that the melting point distribution of the first type of crystalline polyurethane film undergoes a phase change in this temperature range, resulting in a sudden change in free volume. The free volume of the substance becomes larger, and the small water vapor molecules are more easily permeated, which leads to an increase in moisture permeability. The other two types are only the volume change caused by thermal expansion, and the small volume change corresponds to the slow increase in moisture permeability. When the temperature rises from 18°C to 38°C within this temperature range, the moisture permeability of PT10PE10-PU jumps. This is due to the melting phase transition of its crystalline polymer in this temperature range and its relatively high degree of crystallinity [12]. The increase in free volume is larger, and the increase in moisture permeability is correspondingly larger. As the temperature increases, the volume of the polyurethane elastic film will thermally expand. The free volume of crystalline polyurethane changes greatly near the melting point. The increase in the transmission rate of small water vapor molecules results in a large increase in moisture permeability. The change curve of the moisture permeability of the PTPE-PU coated bridge rock and soil with temperature shows that the moisture permeability of PT10PE10-PU is temperature-sensitive. And its temperature sensitivity range is between 25°C–38°C, which is within the optimum temperature range of the human body.

4 Conclusion

The research in this paper is based on differential thermal scanning calorimetry analysis and found that PT10PE10-PU in the PTPE-PU series has obvious crystal melting behavior. The positron annihilation spectrum test found that the free volume of the PT10PE10-PU film suddenly jumped when it was close to the melting temperature. This has obvious temperature sensitivity. This makes the moisture permeability of the coated bridge rock and soil also jump near the crystallization and melting temperature of the soft segment. When the test temperature is 38°C, the moisture permeability is 2950 g/(m^2·d). Finally, it was found that the geotechnical engineering of the hydrostatic coating bridge was 2.5 kPa.

Acknowledgement: The authors would like to extend their thanks to the learning and research platform, as well as the generous financial support provided by the company and the school.

Funding Statement: Indoor hydrothermal experimental study on seepage drainage geogrid clay subgrade under temperature change (No. SQ21008).

Conflicts of Interest: The research topic of this article is independently completed by the author's team, and does not involve any conflict of interest issues.

References

1. Kim, J. H., Lee, H., Lee, J. S., Kim, I. S. (2020). Preparation and characterization of Juniperus chinensis extract-loaded polyurethane nanofiber laminate with polyurethane resin on polyethylene terephthalate fabric. *Polymer Bulletin, 77(2),* 919–928. DOI 10.1007/s00289-019-02771-6.
2. Li, P., Zhang, Q., Chadyagondo, T. T., Li, G., Gu, H. et al. (2020). Designing waterproof and breathable fabric based on polyurethane/silica dioxide web fabricated by electrospinning. *Fibers and Polymers, 21(7),* 1444–1452. DOI 10.1007/s12221-020-9860-5.
3. Bramhecha, I., Sheikh, J. (2019). Development of sustainable citric acid-based polyol to synthesize waterborne polyurethane for antibacterial and breathable waterproof coating of cotton fabric. *Industrial & Engineering Chemistry Research, 58(47),* 21252–21261. DOI 10.1021/acs.iecr.9b05195.
4. Enomoto, M., Omote, Y., Miyajima, M., Yun, C. K. (2021). NIPAM polymer/polyurethane resin films and the moisture transport characteristics of film-treated fabrics. *Textile Research Journal, 91(3–4),* 434–442. DOI 10.1177/0040517520945690.

5. Yu, Y., Liu, Y., Zhang, F., Jin, S., Xiao, Y. et al. (2020). Preparation of waterproof and breathable polyurethane fiber membrane modified by fluorosilane-modified silica. *Fibers and Polymers, 21(5),* 954–964. DOI 10.1007/s12221-020-9562-z.
6. Turan, D. (2021). Water vapor transport properties of polyurethane films for packaging of respiring foods. *Food Engineering Reviews, 13(1),* 54–65. DOI 10.1007/s12393-019-09205-z.
7. Jose, S. K., Soman, M., Evangeline, Y. S. (2021). Quarry fines: An ideal material for the manufacture of foamed concrete. *Asian Journal of Civil Engineering, 2(1),* 105–120. DOI 10.1007/s42107-020-00310-7.
8. Yang, T. (2021). The application of nanocapsule phase change material in the construction of civil engineering. *Arabian Journal of Geosciences, 6(1),* 210–216. DOI 10.1007/s12517-021-07296-9.
9. Nawar, A. H. (2021). Nano-technologies and nano-materials for civil engineering construction works applications. *Materials Today: Proceedings, 2(1),* 55431. DOI 10.1016/j.matpr.2021.01.497.
10. Kosichenko, Y. M., Baev, O. A., Vasilyev, S. M. (2021). Geo-composite drainage material for hydro-technical and civil engineering. *Solid State Phenomena, 6(1),* 65–72. DOI 10.4028/www.scientific.net/SSP.316.1025.
11. Vasilyev, S. M., Kosichenko, Y. M., Baev, O. A. (2021). New types of geo-composite materials for anti-filtration systems. *Solid State Phenomena, 4(1),* 25–32. DOI 10.4028/www.scientific.net/SSP.316.1031.
12. Gaspard, P. (2021). Deterministic and stochastic models. *Solid State Phenomena, 6(1),* 210–230. DOI 10.4028/www.scientific.net/SSP.3-4.97.